Rheology of nano-confined water using a novel Atomic Force Microscope

A thesis submitted towards partial fulfilment of
BS-MS Dual Degree Programme

by

KARAN KAPOOR

under the guidance of

Dr. SHIVPRASAD PATIL

Assistant Professor

Indian Institute of Science Education and Research
Pune

Certificate

This is to certify that this thesis entitled "RHEOLOGY OF NANO-CONFINED WATER USING A NOVEL ATOMIC FORCE MICROSCOPE" submitted towards the partial fulfilment of the BS-MS dual degree programme at the Indian Institute of Science Education and Research Pune represents original research carried out by " KARAN KAPOOR" at "Indian Institute of Science Education and Research Pune", under the supervision of "Dr. SHIVPRASAD PATIL" during the academic year 2011-2012.

Student
KARAN
KAPOOR

Supervisor
Dr.SHIVPRASAD
PATIL

Acknowledgements

I would like to thank all my lab members because of whom the final year experience has been a pleasant one. Special mention goes to Vinod Bhaiya, as we used to call him, who has helped me along every step and without whom most of the electronics developed in our lab would not have happened. Also it's been a joy to work with Vibham with whom I have had many fun moments. Helping each other out and working side by side was a great experience. The members of the adjacent lab, who used to come along and share light moments with us, also deserve a mention. Exchange of equipment was also going on between the two labs, and if something went missing the first place to look was the adjacent lab. Friends with whom I used to unwind after a long day in the lab were a great support throughout the year. I would also like to thank Rapol sir, who gave his valuable inputs whenever we got stuck on a problem. Last but not the least; I would like to thank Patil sir for his support and guidance during the last three years. Detailed discussions with him, and watching him work helped me learn a lot. He has been patient with me even when I went slack in my work and helped me pick up pace again and motivated me. Not to forget all the parties along the way!!!

Abstract

How does water behave when it is confined to slits and pores of the order of its own molecular size?? This question has been asked and debated for decades. The present thesis is a body of work towards the development of a novel technique to answer the above question. We use a quartz tuning fork as a force sensor as it can detect forces as weak as a pico-Newton. We attach a fibre along the length of one of the arms of the tuning fork such that the sharp tip of the fibre protrudes beyond the length of the arm. The other arm of the fork is fixed to a piezo actuator. The fibre tip is then immersed into water in a liquid cell, and is brought close to the bottom surface of the cell, which is atomically smooth freshly cleaved mica. Water is confined between the tip and mica surface as the tip is brought within a few nanometres of the surface. With the help of the actuator piezo the tuning fork is oscillated and a shear force is applied to the confined water column. By recording the change in amplitude and phase of the tuning fork, we get the shear response of the liquid column. Viscoelastic behaviour was observed followed by shear thinning as we approached towards the surface. It is also seen that the range at which these behaviours are observed depends upon the shear frequency and the shear rate applied. This behaviour closely resembles to liquids near their critical points. Further work is being done to verify this analogy between confined liquid and liquid near its critical temperature. If verified this will consolidate all the data so far in the literature and explain the seemingly contradicting results.

Contents

Chapter 1

Introduction

Isaac Newton in the 17^{th} century in his book "Principia" gave the idea of a viscous liquid. According to it, flow is produced in a liquid when a shear stress (σ) is applied to it, the stress being proportional to the velocity gradient (U/d) developed between the layers of the liquid. The constant of proportionality is the coefficient of viscosity (η).

$$\sigma = \eta \times U/d$$

It was only until the 19^{th} century that Navier and Stokes independently developed a three dimensionally consistent theory of liquids, whose dynamics are governed by the Navier-Stokes equations. The fluids that follow these equations are called Newtonian liquids and show purely viscous behaviour.

This idea of liquids held for around two centuries. But with further investigation and study on liquids and the development of new materials, it was known that many liquids do not show a purely viscous behaviour but also show some elastic properties. The idea of liquid partly exhibiting elastic properties was first given by James Clerk Maxwell in the 19^{th} century in a paper where he proposed a mathematical model for such liquids. These viscoelastic liquids are called complex fluids. Toothpaste, ketchup, polymers are some examples of complex fluids. Over time it has been realised that these liquids are not uniform and have micro structures which have a different response time as compared to rest of the liquid, hence the viscoelastic behaviour.

Another interesting case is when a liquid is confined to the dimensions of its molecular diameter. It shows properties much different from its bulk state with the most notable change happening in the characteristic response time of the liquid[1][2]. The behaviour of liquids confined to slits and pores of the order of it molecular diameter has been a point of debate for decades. The liquid of most interest in this regime is water. Water confined to nano

pockets plays a major role in biology. It has been thought of as one of the major factors in structure of bio molecules, with protein folding and stability of intermediate states being one of the top research areas. Water is also a natural solvent for many biological macromolecules. Along with biology, confined water is of interest in chemistry and tribology as well. The effect of hydration processes on the structural and dynamical properties of materials is still being investigated[3]. The nature of confined water can have a huge impact on improving the control of many industrial processes. An immediate industrial application of confined water could be the lubrication industry.

Many groups around the world are working on the problem of confined liquids and there are many contradicting reports on the physical state of confined liquids. There have been results stating nano-confined water shows Newtonian liquid to elastic solid like behaviour. A variety of instruments and techniques have been used to study the dynamics of confined fluids. These include Surface Force Apparatus (SFA), Atomic Force Microscopy (AFM) and new spectroscopy techniques like florescence co-relation spectroscopy.

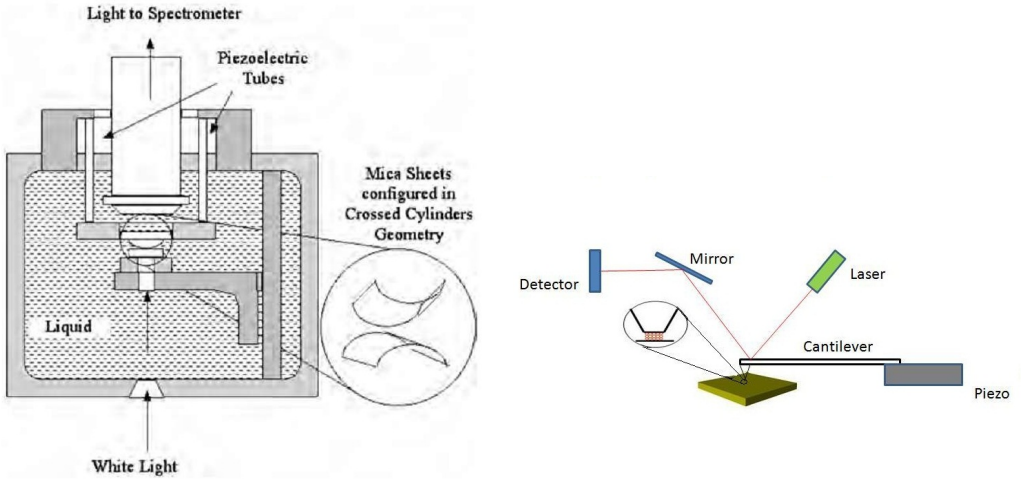

Figure 1.1: Schematic of Surface Force Apparatus and Atomic Force Microscope

The SFA was first developed by D. Tabor, R.H.S. Winterton and J.N. Israelachili in the early 1970's. In a SFA, two surfaces are brought towards and retracted from one another while measuring the interaction between them. One surface is mounted on a piezoelectric tube and the other on weak cantilever spring. The deflection in the spring is used to calculate the interaction force between the two surfaces. The separation between the two surfaces is measured accurately by the use of optical interferometry.

The distance resolution is of the order of 0.1 nm and the force sensitivity is about 10^{-8} N. Due to a weak spring there is a jump-to-contact mechanical instability, which limits the measurements of SFA to film thickness of integer number of layers of molecules.

In Atomic Force Microscope, a sharp tip is attached at the end of a cantilever and is brought close to the sample. The deflection in the cantilever is used to measure the interaction force. S. J. O'Shea along with M.E. Welland and J.B. Pethica was the first ones who used AFM[4] for measuring forces due to confinement at the molecular level. In an AFM the confinement happens between the tip and the surface below. In SFA the geometry of confining surfaces are well defined as compared to AFM, but AFM overcomes the instability of SFA and gives a more comprehensive characterization of the fluid being studied. The main difference in SFA and AFM is the lateral confinement area. In SFA it is few tens of microns and in AFM it is few tens of nanometres. A recent paper[1] based on the measurements using an AFM resolved some of the ambiguities about the behaviour of confined liquids by showing the relation between the behaviour of liquid and the rate of confinement.

The best way to determine the physical state of a material is to measure its shear response. Most of the measurements done are for the normal response of the liquid. Recently a few experiments were conducted for the shear response of the liquid using AFM[2]. But in AFM, due to weak cantilever stiffness there is some normal response of the fluid and hence the true shear response is difficult to measure.

We have designed a novel experimental setup using a fibre tip attached to a mechanically driven quartz tuning fork (qPlus configuration[5]) for shear response measurement of confined liquids. The normal stiffness of our setup can be approximated to infinity. The tuning fork is a very stiff spring hence it has very low thermal noise, high quality factor and high sensitivity of the order of 10^{-12} N. We measure the piezoelectric response of the tuning fork which directly gives us an electrical signal, thus it avoids the use on any optics in our setup.

Chapter 2

Theory

2.1 What is Rheology??

During the 17^{th} century, when Newton gave the concept of viscous liquids, Robert Hooke gave the theory of elasticity for solids. According to it, the deformation in the spring is directly proportional to the tension. As in the case of liquids, not all solids follow Hooke's laws. The Newtonian liquids and Hookean solids form the classical extremes. The behaviour between these two extremes, i.e., showing both viscous and elastic properties is called viscoelasticity. The study of these materials or the study of deformation and flow of matter is called Rheology. The classical extremes are excluded from the scope of rheology.[6]

2.2 Relaxation Time (τ)

An important concept in determining the behaviour of a material is the relaxation time. It's a characteristic property of a material. It is the time taken by the material to respond to an applied stress and bring it back to equilibrium. τ for a Hookean elastic solid is infinite and zero for a Newtonian viscous liquid. The τ for water in liquid state is about the order of 10^{-12} sec.

The scaling of time in rheology is achieved by using a dimensionless quantity called Deborah number (D_e) defined as

$$D_e = \tau/T$$

where T is the time of observation of the deformation process. A high D_e corresponds to solid like behaviour whereas a low D_e corresponds to liquid like behaviour. The time scale of the deformation process also plays a role in the behaviour of the material, as for a liquid with low τ can behave like

an elastic solid for very fast deformation process. This is what happens sometimes with lubricating oils when they pass through gears.

It is suggested that confinement of liquid changes its relaxation time[1][2]. By confining the liquid into smaller regions of the order of nanometres, change of many orders in the relaxation time has been observed using atomic force microscope. The relaxation time of water confined to the dimensions of its molecular diameter has been observed to be in milliseconds[1][2]. This is a change of order of 10^9 from its bulk value.

2.3 Oscillatory Shear

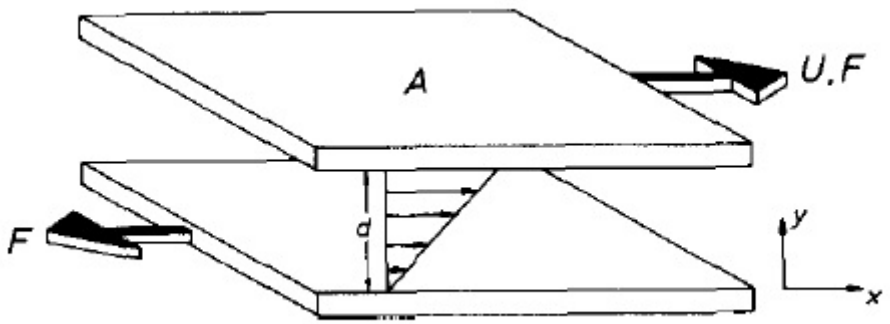

Figure 2.1: Application of a shear force[6]

If a viscoelastic material is confined between two surfaces with separation d, and an oscillatory shear force F, with frequency ω is applied to one of the surfaces with the magnitude of displacement of the surface being X_0. The strain developed on the column of material is given by

$$\gamma = \gamma_0 \times \sin(\omega t)$$

where $\gamma_0 = X_0/d$ The shear stress developed on the column as a result of the force is given by

$$\sigma = \sigma_0 \sin(\omega t + \theta)$$

where $\sigma_0 = F/A$, with A as the area of confinement.

For Hookean solids the phase lag (θ) between stress and strain is zero. And for a viscous Newtonian liquid, the phase lag (θ) is 90^0.

The strain and the stress amplitudes are related by a complex modulus G^* as

$$\sigma_0 = |G^*|\gamma_0 \tag{2.1}$$

G^* is the complex sum of the elastic and the viscous response of the material and is written as

$$G^* = G' + G''$$

The storage modulus G' is the measure of the deformation energy stored in the material during the shear process. Once the load is removed this energy partially or completely compensates for the previous deformation. The loss modulus G'' is the measure of the deformation energy dissipated during the shear process. This energy is dissipated in changing the structure of the material or as heat into the surroundings.

$$G' = |G^*| \cos(\theta) \tag{2.2}$$
$$G'' = |G^*| \sin(\theta). \tag{2.3}$$

If we follow the Maxwell model of a viscoelastic material, which represents the material as a series combination of a spring and a dashpot, we get a relation between the relaxation time and the moduli, as

$$G' = \frac{G_0(\omega\tau)^2}{1+(\omega\tau)^2} \qquad G'' = \frac{G_0(\omega\tau)}{1+(\omega\tau)^2}$$

Where G_0 is a constant. Using the above relations τ becomes

$$\tau = \frac{G'}{G''} \cdot \frac{1}{\omega} \tag{2.4}$$

Another important quantity is the shear rate or strain rate ($\dot{\gamma}$). It is the velocity gradient developed among the layers of the material and is given by the relation

$$\dot{\gamma} = \gamma_0 \omega = \frac{X_0}{d}\omega$$

The reduced shear rate $\dot{\gamma}\tau$ and reduced shear frequency $\omega\tau$ decide the behaviour of the viscoelastic material and will be discussed in the next section.

2.4 Shear rate dependence of Viscosity

For a Newtonian liquid, the viscosity shows no variation with shear rate. But for real liquids, there are certain shear rate induced behaviours.

2.4.1 Shear Thinning and Shear Thickening

The viscosity of liquids has been found to decrease with the increase in shear rate. This behaviour is known as shear thinning. There are many examples

of shear thinning materials around us. Ketchup though resides as a thick liquid but when shaken thins and is easily spread. Toothpaste also, though a highly viscous liquid easily squeezes out of the tube. The variation in the viscosity with shear rate for shear thinning region can be seen the following curve.

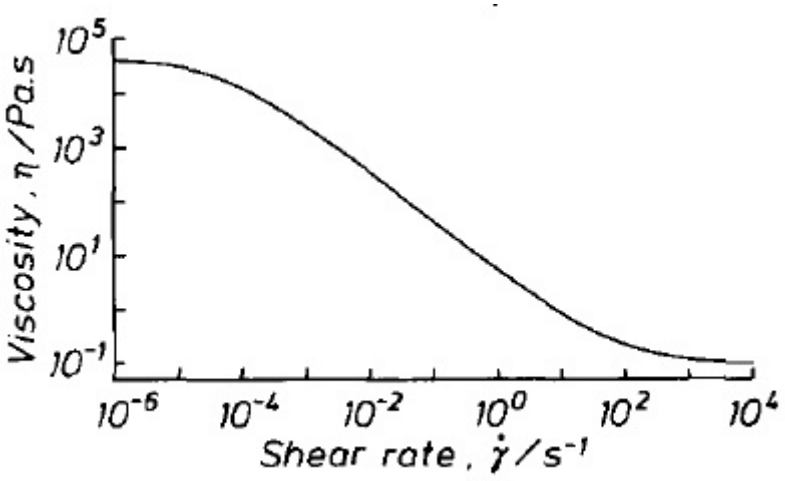

Figure 2.2: Typical shear thinning graph between viscosity and shear rate[6]

Sometimes with the increase in the shear rate, the viscosity increases in a non-linear way. This can be attributed to the rearrangement of the microstructures of the liquid due to the deforming force in such a way that the resistance to flow increases. This behaviour is called shear thickening. In almost all cases where shear thickening is observed, there is a 'shear thinning' region at lower shear rates.

2.5 Factors affecting liquid behaviour

The behaviour of a complex liquid depends upon a number of factors, the shear rate, frequency of shear and the relaxation time being the major ones. Shear thinning is seen when the shear rate ($\dot{\gamma}$) exceeds the inverse of the relaxation time ($1/\tau$), i.e., the liquid it sheared faster than the characteristic response time of the liquid. Linear viscoelasticity occurs at low shear rates when the frequency (ω) of shear exceeds the inverse of the relaxation time. The liquid response can be divided into five regions depending on the shear rate and shear frequency[7]

1. $1 > \omega\tau, \dot{\gamma}\tau$, both the frequency and shear rates are small, the liquid behaves like a Newtonian liquid with constant viscosity.

2. $\dot{\gamma}\tau > 1 > \omega\tau$, the frequency is small but the shear rate is large, we enter a region of quasisteady shear thinning. There are significant distortions in the liquid causing the viscosity to decrease.

3. $\omega\tau > 1 > \dot{\gamma}\tau$, the frequency is large but the shear rate is small, the liquid shows linear viscoelasticity. The distortion is small and hence the liquid response is proportional to the shear rate which leads to viscoelasticity.

4. $\omega\tau > \dot{\gamma}\tau > 1$, both frequency and shear rate are large. Due to the higher frequency, the reversal of the shear rate keeps the distortions small and suppresses shear thinning

5. $\dot{\gamma}\tau > \omega\tau > 1$, both frequency and shear rate are large. Due to huge distortions, the liquid response is reduced suppressing viscoelasticity.

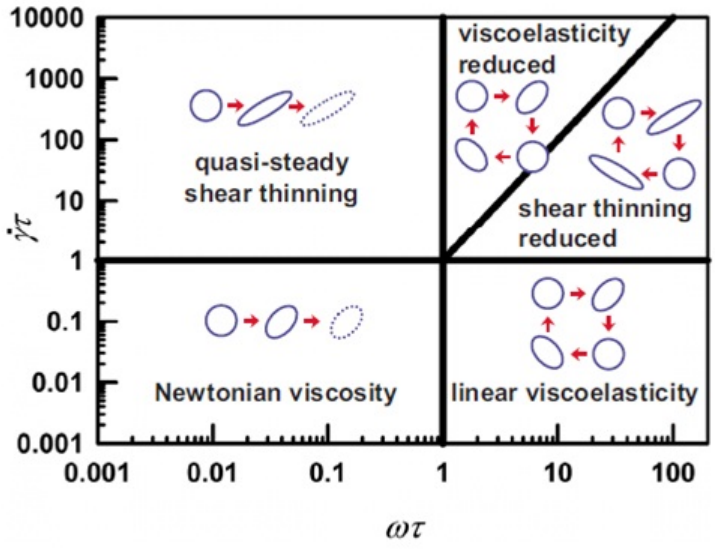

Figure 2.3: Distribution of liquid response into five regions depending on the shear rate and shear frequency[7]

The viscoelastic and shear thinning behaviour are non-equilibrium states on liquid under the influence of a shear force.

Chapter 3

Methods

The goal of the present thesis is to investigate behaviour of nano-confined water. Earlier studies have conclusively shown that water confined to films of thickness less then few molecular diameters have relaxation time τ greater than few milliseconds. The aim of the present instrument development efforts is to study such water using a confinement under a sharp probe ($< 10^4 nm^2$) and shearing this liquid with frequency and shear rates that makes $\dot{\gamma}\tau$ and $\omega\tau$ values greater than 1. The principle experimental parameter to measure non-newtonion behaviour in the experiments is the drag force experienced by the tip confining the water layers. The shear forces or the drag forces involved in such measurements are less than few tens of nano-Newtons. We use tuning forks as a force sensor to both apply the shear and measure the shear response of the liquid.

3.1 Tuning Fork as Force Sensor

The precision of our measurements and the sensitivity of the instrument depend upon the characteristics and sensitivity of our force sensor, Quartz Tuning Fork (QTF).

The QTF has certain advantages as a force sensor. Its high stiffness avoids the thermal noise. It is highly sensitive due to its large quality factor. Piezoelectric property of quartz facilitates the measurement without bulky optical alignments. The signal is an electrical read-out.

The electrical equivalent circuit of a tuning fork (Figure 3.1) is an LCR circuit with a stray capacitance in parallel.

The current generated on the tuning fork due to the piezoelectric property of quartz, and collected by the electrodes on the arms of the fork is of the order of nanoamperes. The signal is amplified and converted to voltage signal

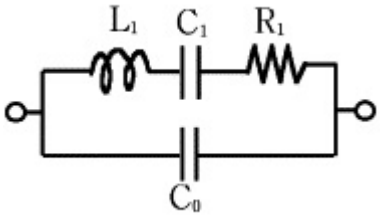

Figure 3.1: Equivalent circuit of a Tuning Fork

with the help of a pre-amplifier circuit. The gain of the pre-amplifier used is 10^7. The Op-amp chip to be used in the pre-amplifier had to be selected such that it was sensitive to detect and amplify the very low signal generated by the tuning fork.

The stay capacitance makes the tuning fork behaviour stay from the lorenzian characteristics as expected from an oscillator. To compensate for the stray capacitance an additional capacitance was introduced in the pre-amplifier circuit.

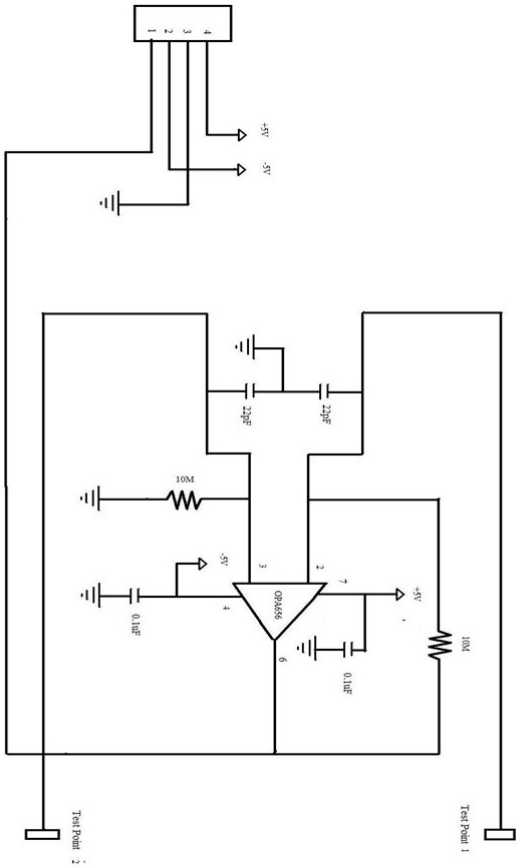

Figure 3.2: Pre-Amplifier Circuit

Giessibl proposed the qPlus design[5] of tuning fork wherein the tuning fork is driven mechanically and the amplitude is measured by monitoring the current through the electrodes. This qPlus configuration is used for the mounting of the tuning fork on the peizo actuator. The actuator is excited using an AC signal of required frequency. This mechanically drives the tuning fork whose signal trough the pre-amplifier is recorded. We have given a frequency sweep to the peizo actuator and recorded the phase and amplitude data for the tuning fork. The characteristic resonance curves with and without the fibre tip attached, are plotted.

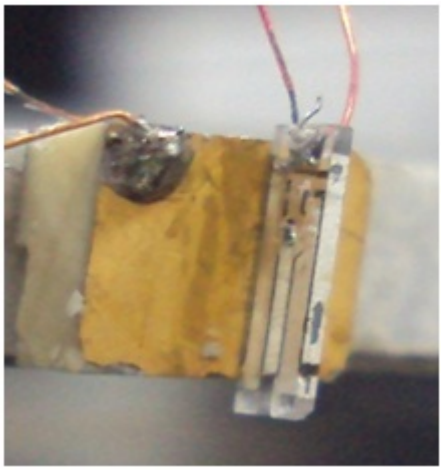

Figure 3.3: Tuning Fork without Fibre

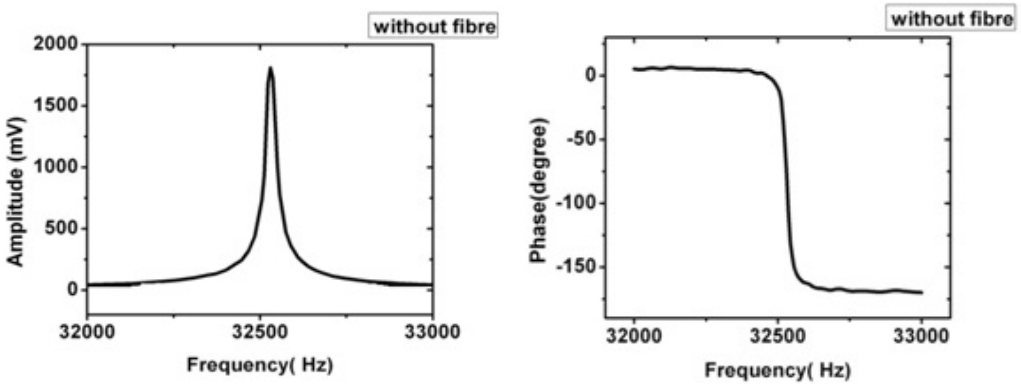

Figure 3.4: Amplitude and Phase curves of Tuning Fork at Resonance

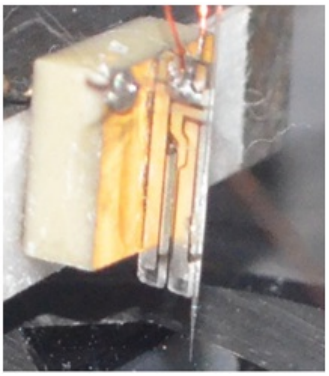

Figure 3.5: Tuning Fork with Fibre tip

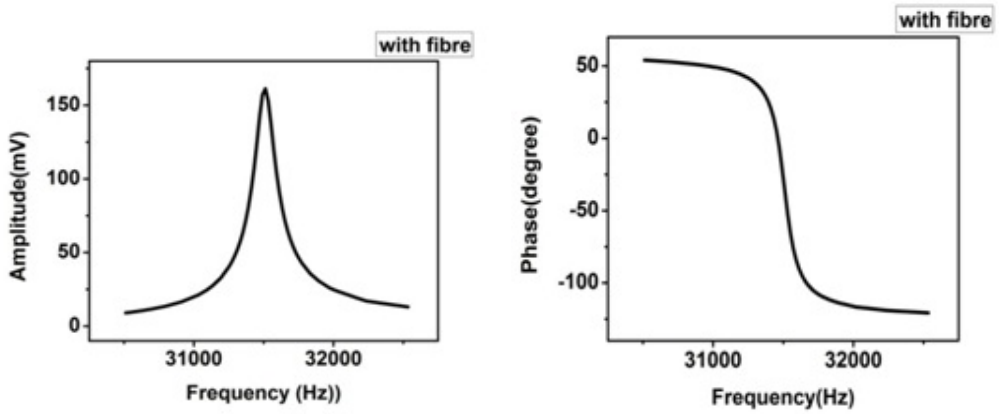

Figure 3.6: Amplitude and Phase curves of Tuning Fork with fibre tip at Resonance

In order to relate the measured current to the prong amplitude the following calculations[5][8] were done to obtain the sensitivity of the tuning fork:

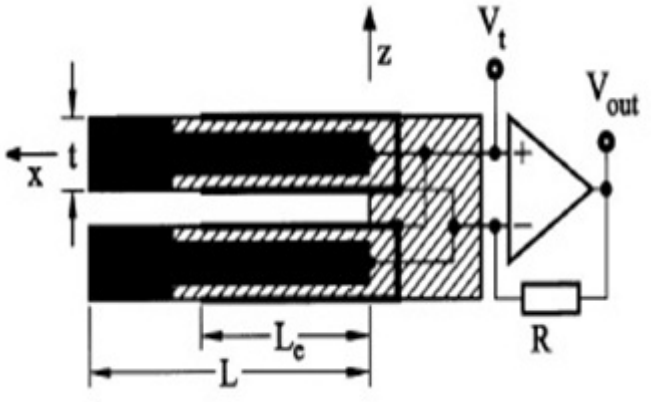

Figure 3.7: Schematic of Tuning Fork[8]

For our geometry of the tuning fork, the spring constant (k) is given by

$$k = 0.25Ew(t/L)^3$$

Where E is the young's modulus, w the width, t the thickness and L the length of one beam of the tuning fork. When a force $F = kz'$, where z' is the deflection along the Z direction, acts on the upper prong. The strain is given by

$$\epsilon(x, z = t/2) = \frac{t}{2}F(x - L)\frac{1}{EJ}$$

Where $J = wt^3/12$ is the moment of inertia for the given geometry

The strain results in the development of stress given by

$$\sigma_{mech} = \epsilon E$$

The stress leads to the charge density

$$\sigma_{charge} = \sigma_{mech} d_{21}$$

Where d_{21} is the piezoelectric coupling constant.

For Quartz

$$\rho = 2650kg/m^3 \qquad E = 7.81 \times 10^{11} N/m^2 \qquad d_{21} = 2.31 \times 10^{-12} C/N$$

We integrate σ_{charge} from $x = 0$ to $x = L_e$ (= length of the electrodes) and $y = -w/2$ to $y = w/2$ and taking into account the equal amount of charge being generated on the lower end of the prong, we get the total charge developed as

$$q/z' = 12 d_{21} k L_e \left(\frac{L_e}{2} - L \right) / t^2$$

For the tuning fork we are using

$$L = 3.5mm \qquad w = 350\mu m \qquad t = 700\mu m \qquad L_e = 3mm$$

The Theoretical sensitivity is given by

$$S_{theory} \approx 2\pi f \times R \times q/z'$$

For $f = 29284Hz$, and $R = 10M\Omega$ in our gain circuit

$$S_{theory} = 343.635mV/nm$$

We use this calculated value of the sensitivity to obtain the amplitude of the tuning fork.

3.2 Probe Preparation

The fibre tip is made using CO_2 laser based Micro-pipette puller from Sutter instruments Model no. P-2000. The fibre is first stripped and placed in the assigned groove in the instrument and then a small portion is heated using CO_2 laser present inside the instrument. The fibre is kept under a constant tension. As the fibre starts to melt due to the heat of the laser, it starts to taper and stretch. When the rate of stretching reaches a set velocity, the laser is turned off and a hard pull is applied to the fibre. Under the influence of the pull, the fibre tapers further and separates into two very sharp tips. We can set various parameters in the instrument to get the desired tip shape.

The following are the parameters

1. Heat: this controls the power of the CO_2 laser. More the heat value the faster the fibre melts. Due to the faster decrease in the viscosity of the glass, higher values of heat lead to longer tapers.

2. Filament: this parameter is used to change the beam profile of the laser. The area to be heated and the distribution of power of the laser on the area can be controlled using this parameter.

3. Velocity: this determines the tip-off point for the hard pull to begin. When the fibre is being stretched under the influence of a constant force, due to the heat the rate of stretching increases with time. When the rate reaches the velocity value set, the heat is turned off followed by the hard pull or the hard pull is executed with the laser being turned off in the middle of the pull, depending upon the value of delay set by the user.

4. Delay: This controls the turning off of the laser. When the separation rate reaches the velocity value, if the delay value is less than 128, then the heat is turned off and the difference (128 - delay) is the time in milliseconds that the instrument waits before executing the hard pull. If the delay value is more than 128, hard pull is executed when the velocity value is reached and the heat is turned off after (delay - 128) milliseconds after the beginning of the hard pull.

5. Pull: It determines the force applied during the hard pull. The more the value the harder the instrument pulls. Longer tapers are formed for higher pull values.

The above parameters were optimised to produce very sharp fibre tips.

3.3 X-Y-Z Nano-positioner

X-Y-Z Nano-positioner[9] has been developed in our lab for AFM purpose. The Z motion is done by an arrangement of peizo tubes. A glass tube is held in its holder with the help of a leaf spring. A peizo tube, called the hammer peizo is attached below the glass tube. The Hammer is used for the coarse Z motion. Inside the glass tube connected to the Hammer glass tube connector is the second peizo tube called the scanner peizo. The Scanner peizo is used for the fine Z motion. The Scanner tube is divided into four quadrants electrically insulated from each other on the outer surface. Each quadrant can be controlled separately, thus the scanner peizo is also used for fine X-Y motion. The sample stage is connected to the scanner peizo.

The hammer peizo is given a saw tooth pulse, with an exponentially rising part and a sharply falling part. During the rising part the glass tube is held fixed by the spring, hence making the hammer peizo expand (or contract) with the centre of the peizo moving in a particular direction. During the sharp falling part, the change is so sudden that the hammer peizo contracts (or expands) back to its normal size in the same position, making the glass tube slide over the spring, hence an overall Z motion. The scanner peizo has

a linear response to voltage and hence the fine motion can be controlled by controlling the voltage to the scanner. For Z motion, all the four quadrants of the scanner have to be provided with the same voltage.

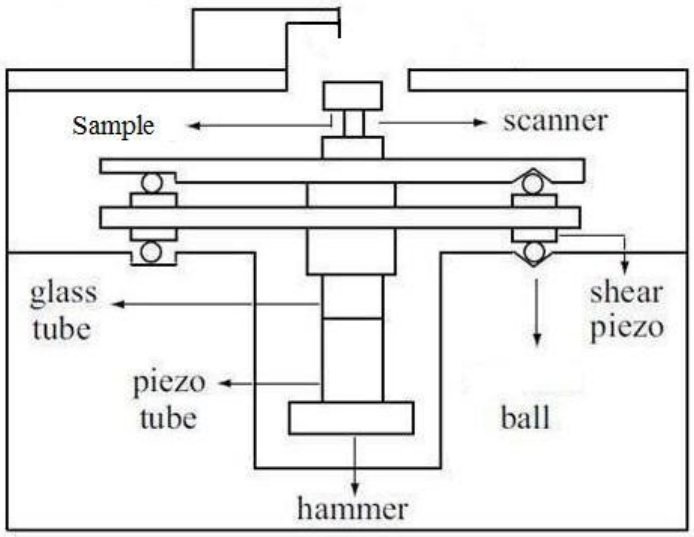

Figure 3.8: Schematic of X-Y-Z Nano-Positioner

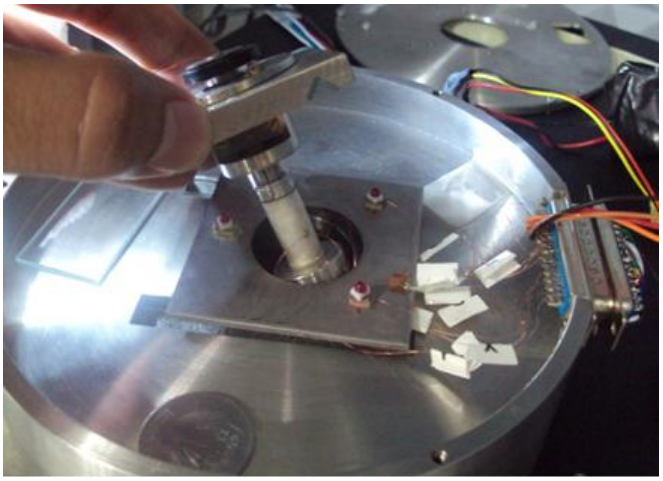

Figure 3.9: X-Y-Z Nano-Positioner

3.4 Calibration of Scanner Peizo Tube

Due to the load of the sample stage (also liquid cell), and with part of the peizo being glued, the response of the peizo is expected to be less than what was given in its datasheet. As the accuracy in knowing the tip sample separation is very important for our experiments, a proper calibration was done of the scanner peizo.

This was done with Michelson Interferometer. A gold plated mirror was glued to the sample stage, acting as the load, and the peizo tube arrangement with the mirror were placed in the place of the movable mirror of the Michelson Interferometer setup. The interference pattern was passed through an iris into a photodiode and seen on an oscilloscope. Voltages (+150 to -150 volts) were provided to the scanner peizo and the number of fringes was counted.

The response of the scanner was found to be $18nm/V$

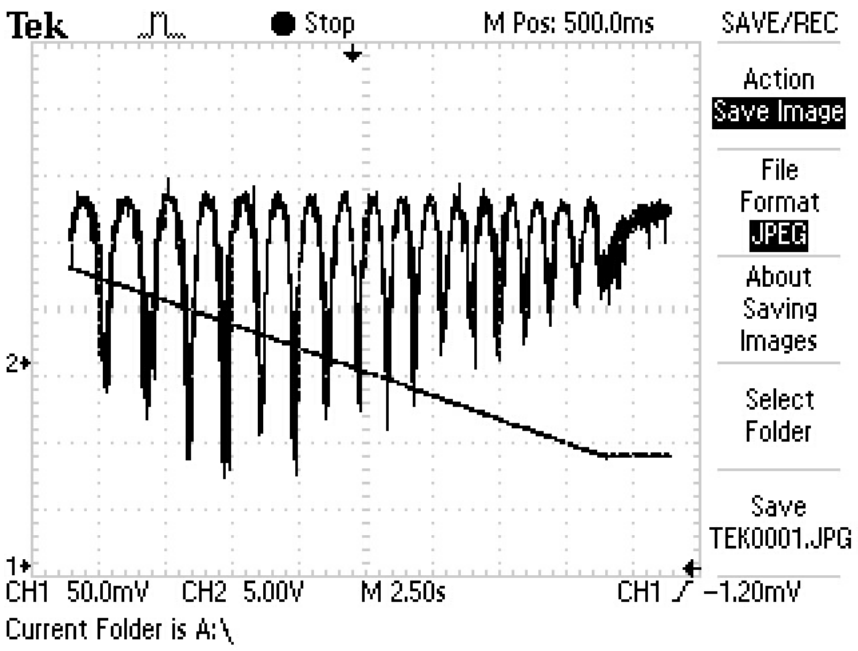

Figure 3.10: Fringes along with the voltage ramp as recorded on the oscilloscope

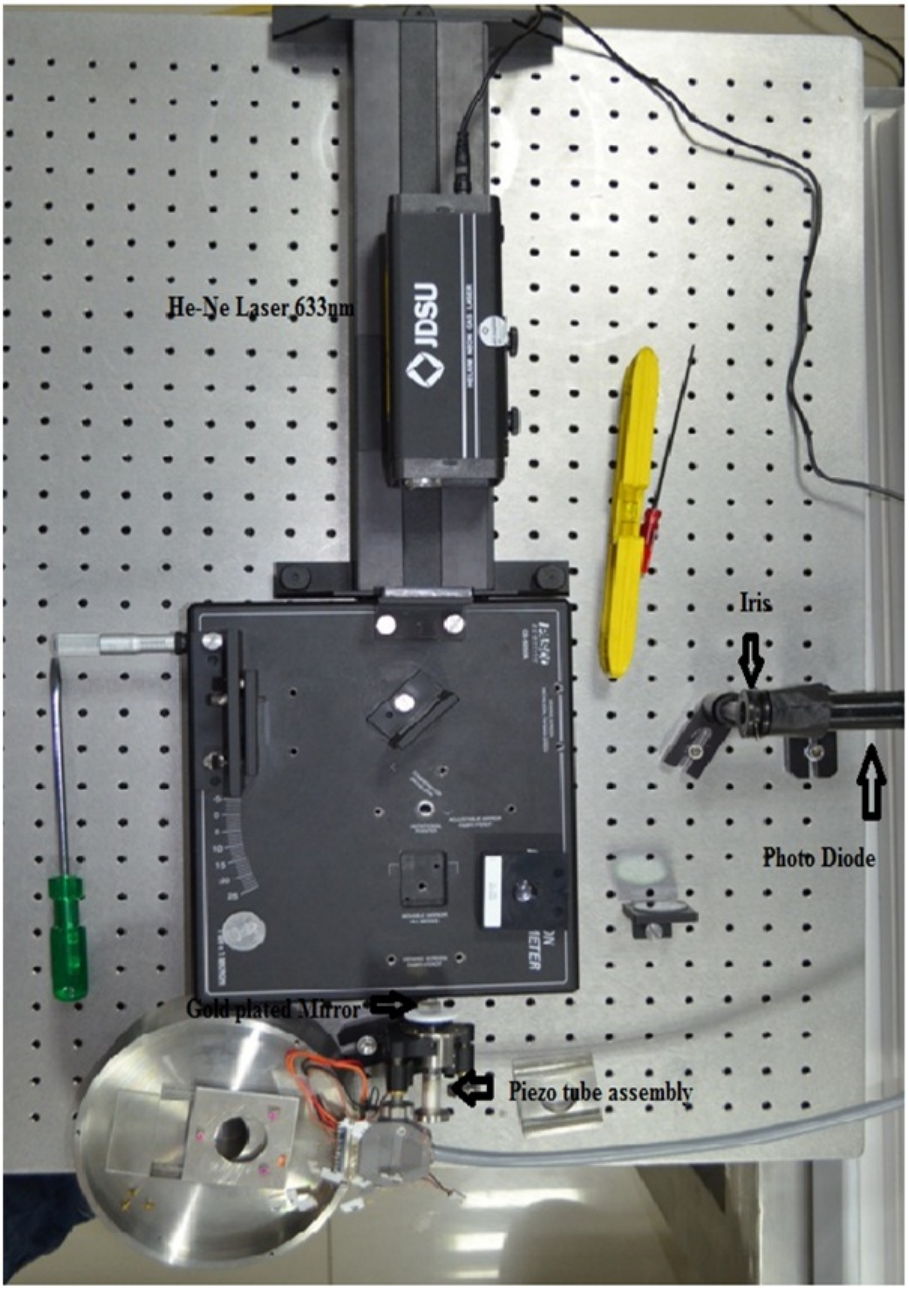

Figure 3.11: Michelson Interferometer set-up for Scanner calibration

3.5 Automation using LabVIEW

Manual approach without damaging the tip is impossible as the distances are of the order of nanometres. Thus a fully automated approach mechanism was developed using LabVIEW software. The program contains the generation of waveforms for the scanner and hammer piezo tubes, auto approach and data acquisition system to obtain the force curves.

The saw tooth pulses for the Hammer peizo were created via the use of logarithmic ramp pattern with the last term being given as zero. The pulses were programmed in such a way that the frequency, the amplitude, the time between two pulses and number of pulses in a burst could be easily controlled and changed anytime. Alone, these pulses are used to control the coarse Z motion. But together with the triangular ramp pattern for the scanner, they form the auto approach mechanism.

During the auto approach, the scanner moves a distance towards the tip in small steps, checking at each step whether the tip is engaged with the sample or not. The interaction region is determined by the signal from the tuning fork and a set-point for the tuning fork signal is determined. If the tip is not it the interaction region for the entire range, then the scanner comes back to its original length and the hammer is moved a distance, a little less than the scanner range, towards the sample. This goes on till the set-point is reached, i.e., the tip is in the interaction region. Once the set point is reached, the control of the program is transferred immediately to the PID controller which tries to keep the tip sample separation constant, by using the tuning fork signal as feedback and giving voltage to the scanner to compensate for the drifts in the system.

To execute this mechanism, first a triangular ramp is given to the scanner peizo and at each step the tuning fork signal is compared to the set-point. The set-point value is user defined and can be set any time before starting the auto approach mechanism. If the set point is not reached during the ramp, a burst of saw tooth pulses is given to the hammer peizo, the parameters of which are set in such a way that the distance moved by the system is little less than the distance the scanner has checked. This pattern of pulses and ramp is run in a loop until the set-point is reached. The moment the set-point is reached, the control of the program jumps out of the loop and is transferred to the PID controller which maintains tip sample separation.

We perform the auto approach in two steps. In the first step the scanner is made to cover the maximum possible distance it can cover, making the approach faster. Once the set-point is reached, the control is not immediately transferred to the PID, but the scanner is contracted back to its original length and the tip disengaged. The approach mechanism is then re-executed,

but this time the distance checked by the scanner is appreciably smaller than before. This is the slow approach and is executed after the first step such that the interaction region is not too far away so that the approach takes less time. Now once the tip is engaged the control is transferred to the PID. This ensures that the interaction region is approached with Z-scanner voltage close to zero.

The approach is done on resonance as there is maximum amplitude change and it is easy to determine when the tip is engaged with the sample. The advantage of the two step approach is that, at the point of engagement the voltage on the scanner peizo is small, making available to us a large voltage range for the scanner to use while collecting data. The final step of the program is to collect data. The PID is disabled and the scanner piezo is given a voltage ramp of the desired range and at each step the amplitude and phase values of the tuning fork are collected and stored on the system for us to analyse later. At each execution of the experiment, the data collected is stored in a different file. During data acquisition the control of the range, the step size and the number of points are user controllable.

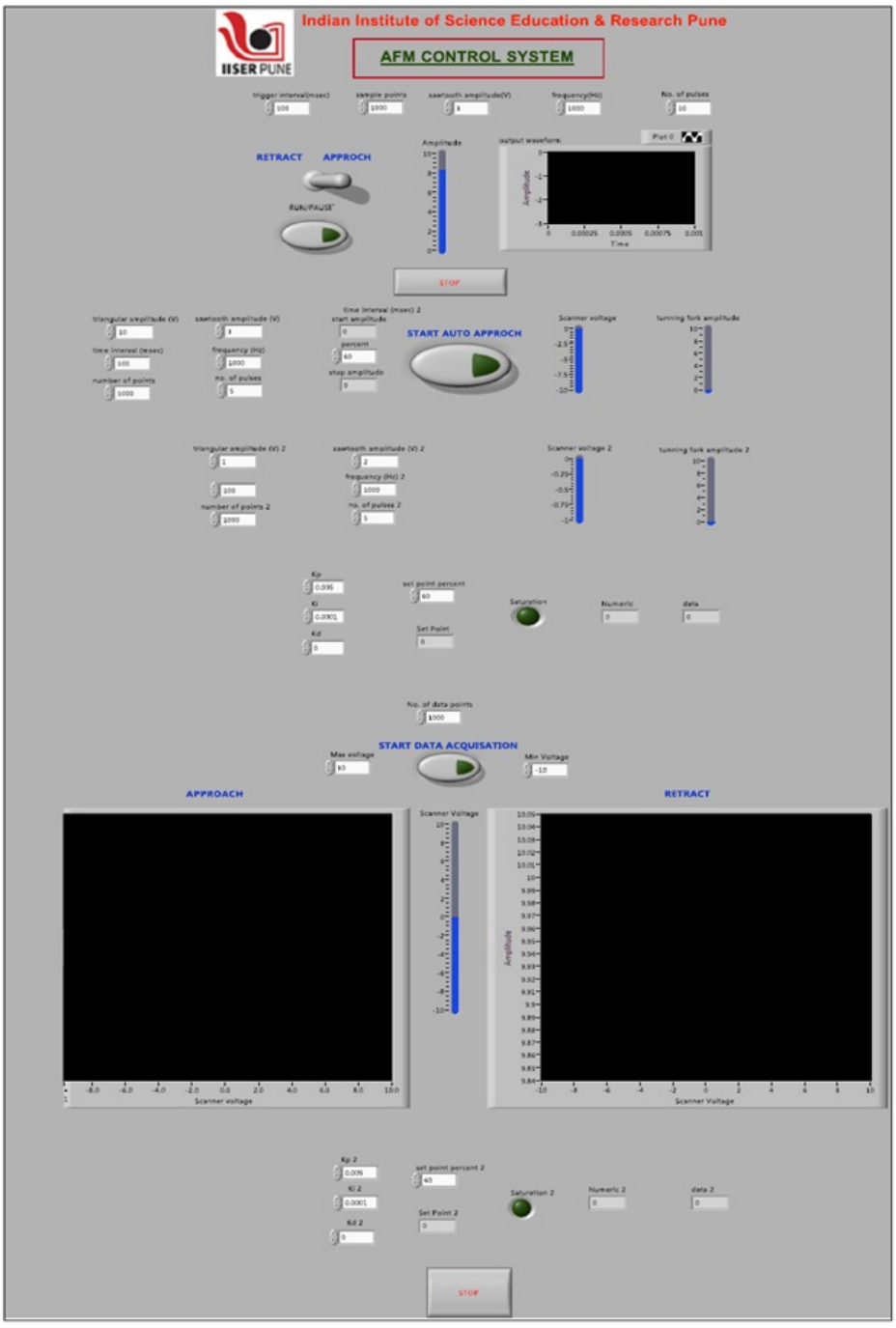

Figure 3.12: The Front Panel developed using LabVIEW

3.6 The Complete Setup

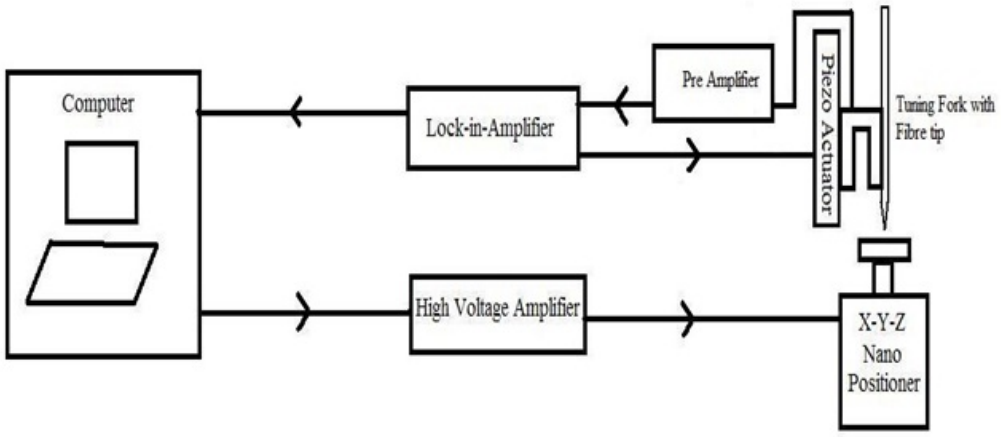

Figure 3.13: Schematic of the Complete Set-up

A fibre tip is attached along one of the arms of a quartz tuning fork with the tapered part hanging in front of the arm. The other arm of the tuning fork is fixed on a piezo actuator such that the fibre tip and the actuator base are parallel to each other. The actuator is mounted on a steel holder, which is fixed to the X-Y-Z Nano Positioner base, thus providing stability to the system. The actuator is excited by an AC signal of the desired frequency from Lock-in-Amplifier, which in turn excite the tuning fork. The current generated on the tuning fork is collected and amplified by a factor of 10^7. The amplified signal is given back to the Lock-in-Amplifier. The Lock-in-Amplifier filters out the noise from the signal and only shows the signal at the driving frequency. It also extracts the amplitude and the phase information from the signal.

The pulses generated using LabVIEW programming were given to home built high voltage amplifier via DAQ card. The amplified signal is then used to drive the hammer and the scanner piezo in the X-Y-Z nano-positioner. On the sample stage we place a Liquid Cell. The cell if filled with purified Millipore water up to a level such that only the fibre tip is immersed in the water and not the tuning fork.

The amplitude and the phase data from the Lock-in-Amplifier are taped into the computer via the DAQ card. At the time of experiments the data values are stored in a file created at each run of the program. A different file

name is generated at each run hence there is no loss due to overwrite of the data.

3.7 Water Confinement Experiments

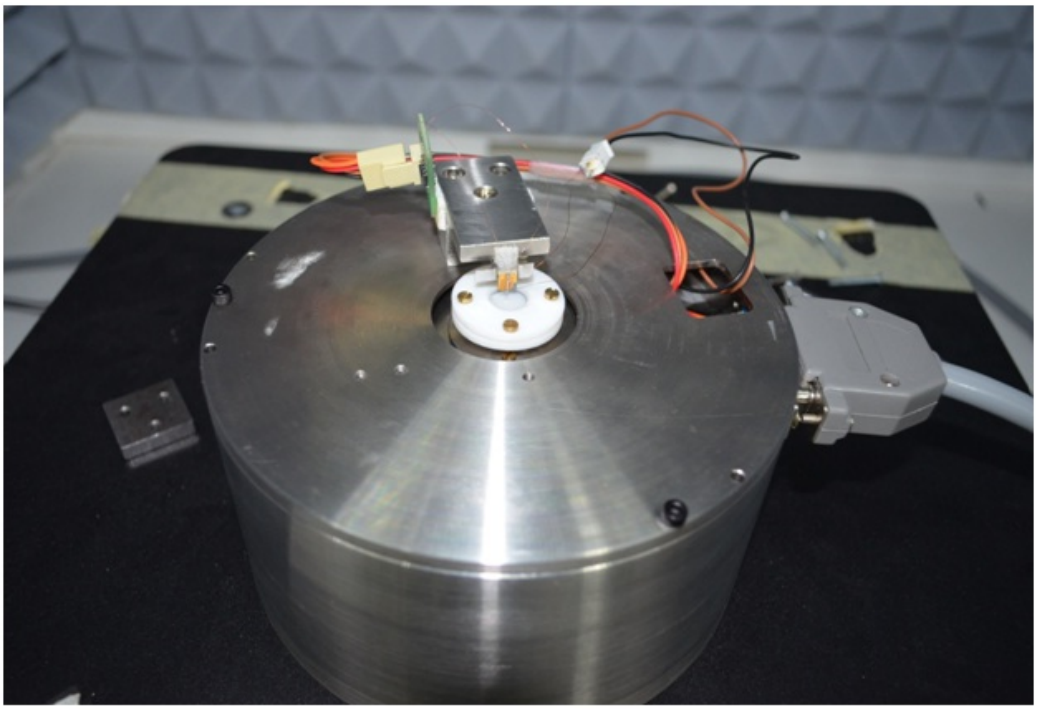

Figure 3.14: Experimental Set-up

Initially the tip is outside the liquid cell, and the tuning fork is excited at its resonance frequency. When the tip enters the water it experiences a drag force, which loads the tuning for and changes its resonance. The change is of the order of a 100-200 Hz. As the tip enters further the drag increases due to increase in surface area in water. We have to keep tracking the new resonance as being at resonance at the time of auto approach is very important. Due to small shift of resonance, the fall in the amplitude is gradual. But when the tip reaches a few nano meters near the surface there is sharp decrease in amplitude due to confinement and also the below surface and tip interaction. When we see the sharp decrease, we retract the probe by one step and start the auto approach.

When the tip is approached, we give the scanner a voltage ramp such that the range of the ramp is big enough for us to go from bulk behaviour to

confinement to hard contact, and small enough with enough number of points such that we do not lose any valuable information. The readings of the tuning fork are recorded during the ramp and analysed. During data acquisition, the time constant of the Lock-in-Amplifier is adjusted so as to minimise the noise without losing out on information. The time between acquisition of two data points has to be adjusted according to the time constant of the Lock-in-Amplifier.

Once the tip is in the interaction region, we can change the driving frequency and take off-resonance data. We have collected data on range of driving frequencies. The Lock-in converts the signal into a range of 10 Volts according to the sensitivity value set. Matlab codes have been written to analyse the data. The sensitivity values of the tuning fork as well as the Lock-in and the calibration of the scanner have been incorporated in the program to give us data in terms of the tuning fork amplitude and the tip surface distance in nano-meters. The data is then plotted.

Chapter 4

Results

Figure 4.1 (a) and (b) show force curves in air for the tuning fork on resonance with the fibre tip attached

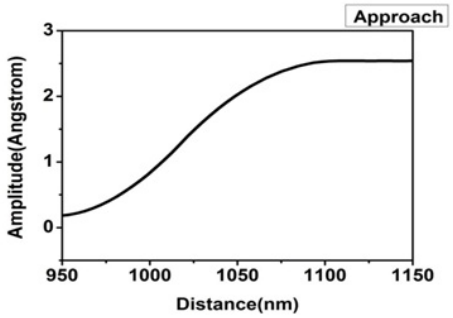

(a)

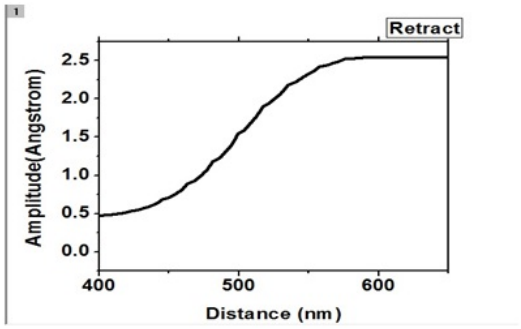

(b)

Figure 4.1: Amplitude vs Distance curve in air (a) approaching a surface (b) retracting from a surface

Zero for the separation is not defined; the X-axis values start from an arbitrary number. The interaction range in air is up to 200 nm.

The following force curves are taken under water at resonance. It is clearly visible that the interaction distance has been reduced by a considerable amount.

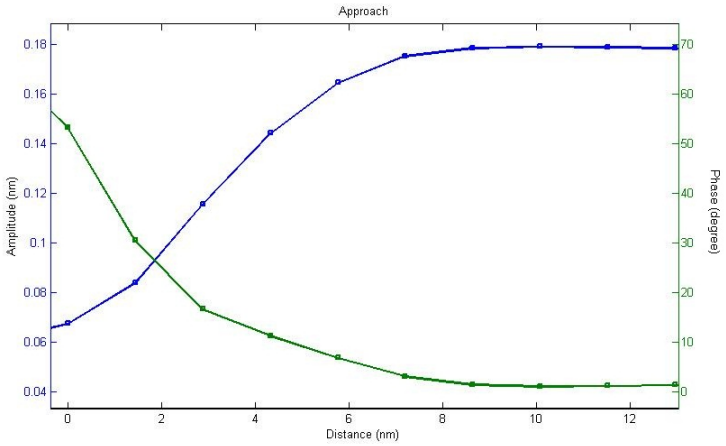

(a)

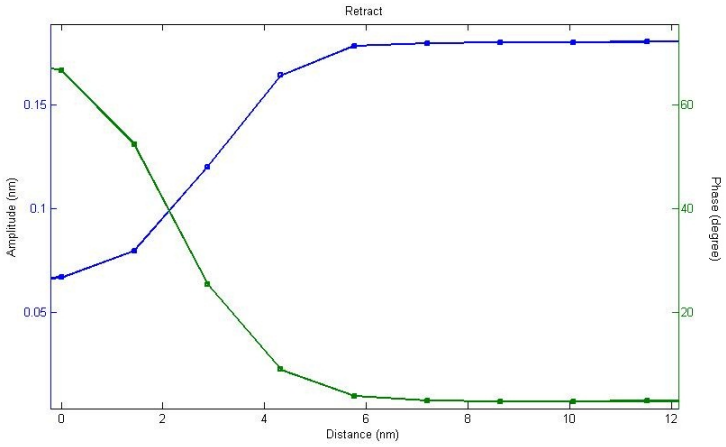

(b)

Figure 4.2: Force curves in water (a) approaching a surface (b) retracting from a surface

Following off-resonance curves of the relative change in amplitude, and the phase with the separation between tip and freshly cleaved mica surface

The confinement happens from $0 - 10$ nm range. Roughly the volume of confinement is 10^{-21} litres. We calculate this by assuming tip area to be $10^4 nm^2$.

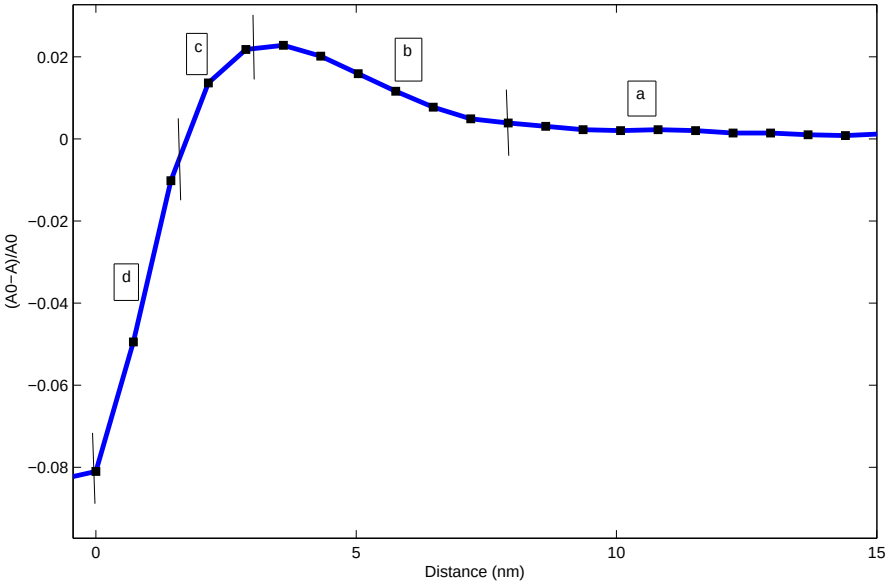

(a) Relative change in amplitude vs Distance

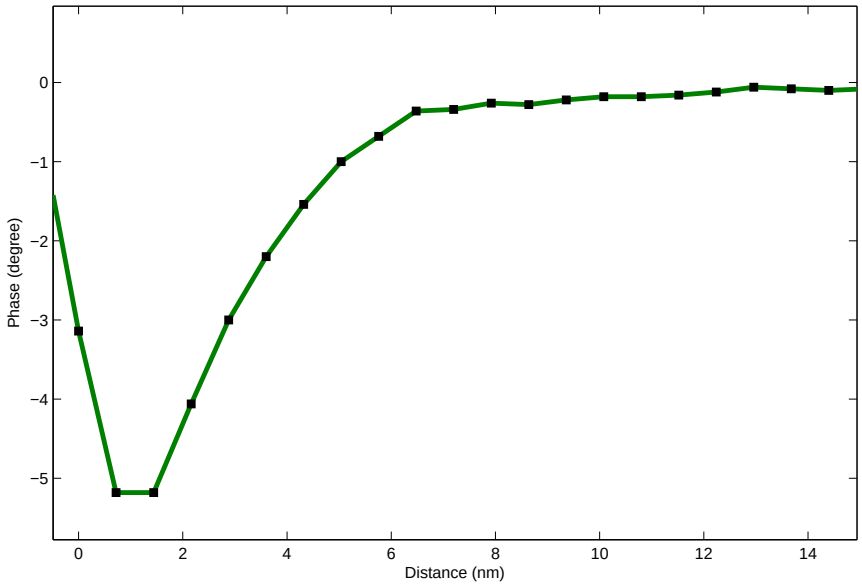

(b) Phase vs Distance

Figure 4.3: Off resonance force curves in water at $f = 18kHz$

After reaching the separation of the tip and surface of the order of few 100 nanometres, we perform off resonance experiments to determine the drag force at different frequencies and amplitudes. Figure 4.3 shows a typical shear force curve obtained at $f = 18kHz$ and drive of 2 volts. If the viscous drag is more than the bulk value it is expected that the amplitude of the tuning fork will decrease. Positive change in amplitude will indicate reduced viscosity. The Y -axis of the figure is $(A_0 - A)/A_0$. Positive ΔA means the amplitude is decreasing. Negative vale of ΔA corresponds to viscosity lower than the bulk value.

We can clearly see three regions in the force curve of confined water. The region (a) where the separation is still large, there is no change in the amplitude of the tuning fork. The behaviour is Newtonian liquid like.

Going closer we enter region (b). There is increase ΔA, i.e., there is decrease in the amplitude of the tuning fork. This can be related to increase in the effective viscosity. This region shows viscoelastic behaviour.

In the region (c), there is sharp decrease in ΔA, i.e., increase in the amplitude of the tuning fork. But the amplitude is still greater than the free amplitude. The viscosity of water has started to decrease and is approaching the bulk value. This region is of reduced shear thinning.

In the region (d), the ΔA becomes negative. The amplitude of the tuning fork is more than its free amplitude. This indicates viscosity values less than the bulk value. This is the region of shear-thinning.

The following is the force curves of confining water at different frequency showing the frequency (ω) dependence of the three regions in the curves.

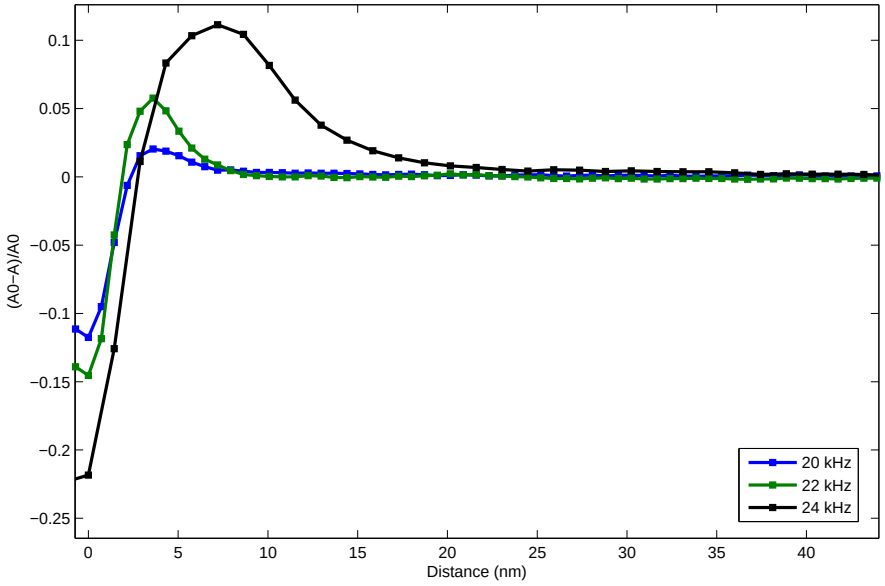

Figure 4.4: Force curve showing frequency dependence behaviour of confined water

Chapter 5

Discussion

The importance of nano-confined water in nature is very well known but the debate on its behaviour has been long going. Several sets of experiments have been performed to determine the behaviour of nano confined water, but have resulted in lot of ambiguity. There is a lot of disagreement among the results of various groups.

Experiments done by J. Klein[10][11][12] group have reported near bulk viscosity of confined water. They have used a Surface Force Apparatus (SFA) and confined water between two mica surfaces. The viscosity measured was within a factor of three of the bulk viscosity. An interesting thing in their experiment was the region where the jump-in-contact takes place. It is seen that there is reduction in the viscosity though it remains within a factor of three of the bulk value. The decrease in viscosity is proportional to the jump-in time, i.e., the faster the jump the lower the viscosity[10].

There are experiments that show contrary results as well. The group of Steve Granick uses SFA for these measurements and has seen increase in effective viscosity with the decrease in separation[13][14]. Also experiments using Atomic Force Microscope (AFM) have also been performed by various groups[2][15][16][17][18]. They have also shown an effective increase in the viscosity confined water. In some cases, the loss modulus and the storage modulus is calculated and viscoelastic behaviour of confined water is implied[2][15][13].

A recent PRL[1]on confined water had resolved some of the ambiguities by showing that the behaviour is linked with the rate of confinement. The group used small amplitude AFM technique for the study. They have shown that above a certain rate of confinement, water starts showing elastic properties. When the confinement is an integral multiple of the molecular diameter, water has solid like behaviour else in a high viscous liquid state. The observation where with the increase in confinement from a few nanometres, there

is decrease in viscosity is still not explained.

In our experiments, we can see three regions in the curve. When the separation is large, there is no change in the viscosity of water and it behaves like a Newtonian liquid as in bulk state. Then there is a gradual decrease in the amplitude of the tuning fork, accompanied by a phase change. This decrease can be put to as a result of viscoelastic behaviour of the water film. Then as we approach closer there is a sharp decrease in the resistance to the flow. There is increase in amplitude with a recovery in phase pointing towards shear-thinning behaviour.

It has been observed that the relaxation time (τ) of confined water increases by many orders from its bulk state. The relaxation time of the confined water is found to be of the order of millisecond[1][2]. An analogy can be formed between confined liquids and liquids near their critical point. As the liquid nears its critical temperature, coupling between fluctuations of density and velocity causes a huge change in the fluctuation relaxation time[7]. We propose that during confinement, the liquid tries to order itself between the approaching surfaces and there are local density fluctuations having longer relaxation times.

As discussed earlier, when we shear a liquid faster than the fluctuations, the relaxation depends upon the values of $\omega\tau$ and $\dot{\gamma}\tau$. Depending on their values five regions can be created in the $\omega\tau - \dot{\gamma}\tau$ space as shown in Figure 2.3.

As we reach confinement, due to the increase in τ, the quantity $\omega\tau$ acquires a significant value. This pushes the liquid into the viscoelastic region. This corresponds to the region (b) in our graph. As we further decrease the confining volume, the ratio of X_0 - the shear amplitude, and d - the separation, increases. This increases the shear rate $\dot{\gamma}$, and the condition $\omega\tau > \dot{\gamma}\tau$, the region of reduced shear thinning. This corresponds to the region (c) in the graph. With further decrease in the separation the liquid is pushed into the region of shear-thinning as the condition $\dot{\gamma}\tau > \omega\tau > 1$, corresponding to the region (d) in our results. We can also see the dependence of the regions on ω in our results. The increase in ω will push the liquid into the reduced shear-thinning region and the viscoelasticity is enhanced. In tuning fork, there is slight increase in the amplitude which increases the amplitude X_0 of the force thus also enhancing the shear-thinning region as is seen in our results.

The dynamics of confinement happens at the tip water junction, whereas we measure the amplitude and the phase at the tuning fork fibre junction. The amplitude of the tuning can be easily concluded to be proportional to that of the fibre with the proportionality constant given by the ratio of their respective spring constants. But the phase relationship is more complicated

with added complexity due to the viscous drag faced by the part of the fibre immersed in liquid. To determine the phase relationship we have to solve the problem of coupling of a harmonic oscillator with a damped harmonic oscillator.

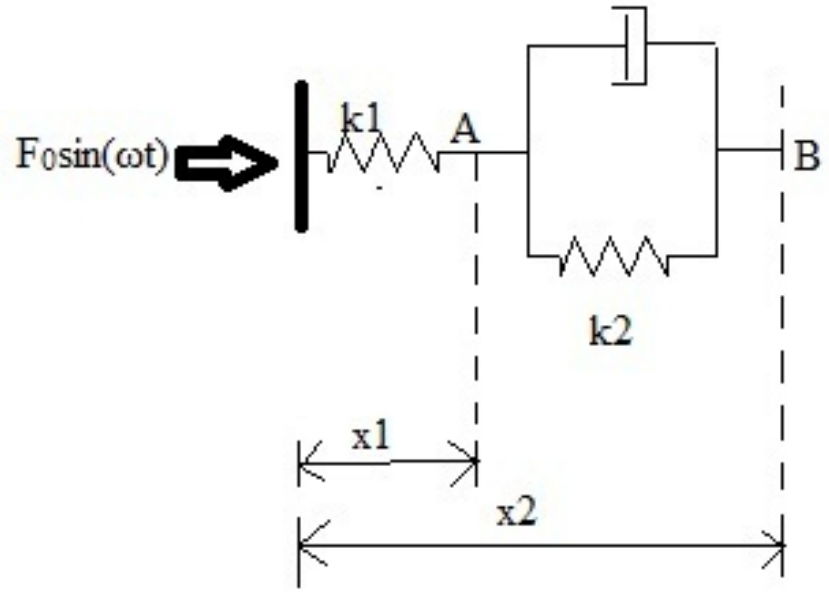

Figure 5.1: Mechanical model of tuning fork and fibre system

Here the spring $k1$ represents the tuning fork and $k2$ the fibre. The dash-pot signifies the viscous damping caused due to water on the fibre. A sinusoidal force $F_0 \sin(\omega t)$ is applied through the actuator peizo on the tuning fork. We measure the amplitude and force at point A, and we want to get information of the amplitude and especially phase at point B.

If we are able to accurately get the phase relation, then we will be able to calculate the storage and the loss moduli G' and G'' from the complex modulus (G^*) of viscoelasticity using

$$G' = |G^*| \cos(\theta)$$

$$G'' = |G^*| \sin(\theta).$$

And further we would be able to get information on the value of τ at the different points of the graph and plot τ with the confinement distance

$$\tau = \frac{G'}{G''} \cdot \frac{1}{\omega}$$

This will further strengthen our claim of combined viscoelasticity and thinning, and give us a better understanding of the dynamics of confinement of liquids.

From our observations we conclude that there is strong dependence on the shear rate and shear frequency on the behaviour of a confined liquid. This regime consolidates all the experimental results thus far and explains the ambiguities in the results, thus taking a major step in the direction of understanding the behaviour of confined liquids. But further work needs to be done to support this rather bold claim. We are now planning to explore all the regions in the $\omega\tau - \dot{\gamma}\tau$ space. This can be done by taking measurements at different frequency values and different excitation voltages, i.e., different X_0 values. If we see a jump from one region to another for a particular ω or X_0, then it is possible to calculate the effective τ from the readings.

Further we have planned to modify our current setup and combine it with Florescence Co-relation Spectroscopy (FCS). With the new instrument, we want to measure the mobility of a confined liquid under the influence of a shear force. The design of the new instrument is ready and we have also sent the parts for manufacturing. We plan to setup and get the Instrument running in the coming month.

References

[1] Shah H. Khan, George Matei, Shivprasad Patil and Peter M. Hoffmann, Phys. Rev. Lett. 105, 106101 (2010)

[2] T. D. Li and E. Riedo, Phys. Rev. Lett. 100, 106102 (2008)

[3] John L. Finney, Hydration Processes in Biological and Macromolecular Systems, Faraday Discussions, NO. 103, (1996)

[4] S.J. O'Shea, M.E. Welland, J.B. Pethica, Atomic force microscopy of local compliance at solidâĂŤliquid interfaces, Chemical Physics Letters, Volume 223, Issue 4, 24 June 1994, Pages 336-340

[5] Franz J. Giessibl, Appl. Phys. Lett. 73, 26, 3956(1998)

[6] Barnes, Hutton, Walters, An Introduction to Rheology,Elsevier Science Publishers (1989)

[7] Robert F. Berg , Michael R. Moldover, Minwu Yao and Gregory A. Zimmerli , Phys. Rev. E, 77, 041116 (2008)

[8] Franz J. Giessibl, Appl. Phys. Lett. 76, 11, 1470(2000)

[9] Shivprasad Patil, George Matei, Hang Dong,Peter M. Hoffmann, Mustafa Karakose and Ahmet Oral, Rev. Sci. Instrum. 76, 103705 (2005)

[10] U. Raviv, P. Laurat, and J. Klein, Nature 413, 51 (2001)

[11] U. Raviv and J. Klein, Science 297, 1540 (2002)

[12] U. Raviv, S. Perkin, P. Laurat and J. Klein, Langmuir 20, 5322 (2004).

[13] Y. Zhu and S. Granick, Phys. Rev. Lett. 87, 096104 (2001)

[14] Ashis Mukhopadhyay, Sung Chul Bae, Jiang Zhao, and Steve Granick, Phys. Rev. Lett. 93, 236105 (2004)

[15] M. Antognozzi, A. D. L. Humphris, and M. J. Miles, Appl. Phys. Lett. 78, 300 (2001)

[16]] S. Jeffery, P. M. Hoffmann, J. B. Pethica, C. Ramanujan, H. O. Ozer, and A. Oral, Phys. Rev. B 70, 054114 (2004)

[17] T. D. Li, J. P. Gao, R. Szoszkiewicz, U. Landman, and E. Riedo, Phys. Rev. B 75, 115415 (2007)

[18] R. C. Major, J. E. Houston, M. J. McGrath, J. I. Siepmann, and X. Y. Zhu, Phys. Rev. Lett. 96, 177803 (2006)